The mechanism of cardiac tropomyosin transitions on filamentous actin as revealed by all atom steered molecular dynamics simulations

Michael R. Williams,[†,§] Jil C. Tardiff,[‡,¶] and Steven D. Schwartz[*,†]

†*Department of Chemistry and Biochemistry, The University of Arizona, Tucson, AZ 85721*

‡*Department of Medicine, The University of Arizona, Tucson, AZ 85724*

¶*Department of Cellular and Molecular Medicine, The University of Arizona, Tucson, AZ 85724*

§*Current address: Center for Intergrative Chemical Biology and Drug Discovery, University of North Carolina, Chapel Hill, NC 27599*

E-mail: sschwartz@email.arizona.edu

Contents:

Computational Methods

The computations reported here employ a model, which was described by Williams et al.[1] Recent refinements included in that iteration included the modification of the Tm overlap region and the addition of a second Tm and troponin complex on the opposite side of the actin filament. Li et al.[2] and Orzechowski et al.[3] address an ongoing debate as to the structure of the overlap region, and we have followed their results. At the overlap, they found that the helical pitch of the coiled–coil is removed such that the double strand straightens at the termini. Since our model contains cardiac troponin (cTn), resulting in decreased distance between actin and Tm, our first task was to recreate an overlap in accordance with this most likely structure. To create sections of the Tm termini with no helical pitch around each other, DiscoveryStudio was employed. Their structures of "straightened" Tm overlapping termini were created with only Tm and actin, while our model contains cTn, which results in a reduction of distance between Tm and actin. The our straight α–helices were then aligned using VMD 1.92[4] to the remaining Tm segments using the published structure[3] as both a scaffolding for orientation and guide for relative distances. The Tm coiled–coil dimers were then minimized under implicit solvent conditions before being added to the actin filament. Once the helical pitch of the Tm termini was eliminated from the full atomistic model, the new overlap resulted in a more stable region in which the distance between termini of the two chains of an individual dimer was consistent over long simulation periods.

To increase the productivity of the full atomistic CTF model, a second set of Tm and the cTn complex were added. The second set of Tm chains and cTn complex was added by aligning the original set onto the "empty" polymerized chain of globular actin subunits. The second set allows for the simulation of a second CTF model without the full computational cost of running an entire other simulation. The addition is also relevant because the second side is present naturally; thus, the model now represents a full unit cell of the CTF. The resulting modifications result in the model consisting of 30 actin subunits, with 8 total chains of Tm (2 separate cables of overlapping coiled–coil dimers), and 2 full cTn complexes. The

model was then solvated, minimized, heated and equilibrated.

The following is the same computational setup protocol that was implemented in our previous model simulations.[1] Model preparations were produced utilizing VMD 1.92.[4] The Solvate feature of VMD 1.92 was used to create a full TIP3P water box with the box size is set to be 15 Å away from the protein in all directions. Water molecules could not be placed within 2.4 Å around the protein. The Autoionize feature was then used to place ions in the solvent box to both neutralize and add a solvent concentration of 0.15 M KCl. The resulting solvated CTF model has just over 5 million atoms in total. The CTF model is then minimized for 5,000 steps using NAMD 2.12[5] with the CHARMM 27 force–field parameters.[6] Periodic boundary conditions were used with a fixed box size. The wrapAll feature was turned on. The particle mesh Ewald (PME) method of calculating long-range electrostatic interactions was used, whereas the Van der Waals interactions were cut off at 12 Å. The PME grid spacing was set to 1.0 Å, and the tolerance was set to 10^{-6}. The SHAKE algorithm was used to constrain the hydrogen bond lengths with a tolerance of 1.0^{-8} Å. The CTF model was then heated to 300 K using NAMD 2.12[5] with the CHARMM 27 force–field parameters while increasing the temperature 1 K every 1000 fs. Since the system was only 298 K when 300 ps was reached, an additional 10 ps was simulated in which the temperature was rescaled to 300 K ever 1000 fs, therefore, the temperature was able to reach 300 K. During equilibration, the zeroMomentum function was used to remove the center of mass (COM) drift that can occur due to the implemetaion of the PME method. The heated model was equilibrated in NAMD 2.12 along with the CHARMM 27 force-field parameters for 690 ps in the canonical (NVT) ensemble. A 1 fs time step was used and data was saved every 5 ps. Randomly generated initial velocities were scaled to 300 K.

Steered molecular dynamics (SMD) is a enhanced sampling method the allow the sampling of rare events. SMD is utilized as a potential of mean force calculation to find the free energy of a transition from the calculated work.[7,8] SMD implements a virtual atom that is attached to a virtual spring, which is attached to the COM of the atoms that the enhanced

sampling is needed. When a constant velocity is applied to the virtual atom in the targeted vector, the atoms attached to the other end of the virtual spring feel the applied force due to the spring elongated.[7] The 28 locations are the quasirepeats of Tm that interact with F–actin, since there are seven quasirepeats per a single coiled–coil dimer of Tm and there are 4 sets on the CTF model. For each of the quasirepeats, the backbone atoms (the amine nitrogen, the carboxyl carbon, oxygen, and α–carbon) of 26 amino acids per single Tm chain of the dimer are selected for each SMD site. Therefore, the COM of 208 total atoms per quasirepeat will be attached to the virtual spring that will be pulled during SMD from their original starting location of the equilibrated structure to the COM for the same atoms on the recreated endpoint locations.

To create our target closed position endpoints, Cryo–EM structures were utilized. von der Ecken et al.[9] not only proposed the azimuthal transition, but also deposited the PDB entry 3J8A to the protein database that contained a short five subunit actin filament with the Tm in the closed position. Using this PDB entry as a template, the structure was aligned using the three middle subunits, to each of the actin subunits of our full atomistic CTF model using VMD 1.92.[4] Once the aligned coordinates were saved, a recreation of the CTF model with the location of the PDB entry 3J8A's tropomyosin could be made. von der Ecken et al.[10] also published a different proposed structure of Tm in the closed position (PDB entry 5JLH), and using the same alignment technique as before, a recreation of the CTF with their Tm positioning was produced. From the previously described endpoint structures for the closed positons of Tm, the 28 different SMD pulling locations along the Tm chain were created. The vector used to pull on the virtual atom for each pulling site is calculated as the difference between the ending and beginning positions of each COM. Table 1 shows the directionality of the 3 different transitions.

Since there is an unknown mechanism of breaking the actin Tm interactions, another method of SMD tested was to pull the Tm perpendicular from the F–actin. This is in the opposite direction of the electrostatic interactions. The first vector was calculated as

the vector between the lower and upper α–carbons of the coiled–coil residue pairs of the Tm chain that is perpendicular to the actin plane from which Tm is being pulled. After the perpendicular pull is complete, a second step of SMD pulling was applied in the same manner as the original single directional pulling, except the beginning position for the vector is the elevated position of the COM.

In order to compare the various possibilities for directions of Tm movement, free energy is calculated from work. The work done on each SMD virtual spring is calculated by the standard definition:

$$W_{0\to t} = \int_0^t F_{t'} \bullet v dt' \tag{1}$$

where W is the total work, k is the spring constant of the virtual spring, v is the velocity at which the virtual atom is pulled, t is time, and F is the force that the spring feels. Jarzynski's equality states that the nonequilibrium ensemble average work is equivalent to the equilibrium free energy of the process with sufficient ensemble coverage and weakness of perturbation.[8]

$$\left\langle e^{\beta W} \right\rangle = e^{\beta \Delta G} \tag{2}$$

The β is the inverse temperature, the W is the work, and the ΔG is the change in free energy. To improve the accuracy of the sampling, the cumulant expansion can be used.[7]

$$\langle W \rangle = \langle W_t \rangle - \frac{\beta}{2}\left(\left\langle W_t^2 \right\rangle - \langle W_t \rangle^2\right) + ... \tag{3}$$

The second order cumulant expansion has been show to effectively enhance PMF calculations with SMD simulations.[7]

Table S1: Velocity, time, and total energy for the three SMD transition types. The constant velocity applied to the virtual spring for each of the SMD methods is shown. The time each transition required to reach the endpoint is show for each of the SMD methods. The total energy for each transition required to reach the endpoint are show for each of the SMD methods.

SMD method	Constant velocity (Å/fs)	Azimuthal time (ps)	Angled time (ps)	Longitudinal time (ps)	Azimuthal total energy (kcal/mol)	Angled total energy (kcal/mol)	Longitudinal total energy (kcal/mol)
SMD	0.0005	65	87.5	87.5	1646.6	2039.9	1985.1
2 staged SMD	0.0005	65	85	85	1556.4	1813.0	1736.6
Slower SMD	0.00005	450	750	750	336.7	460.0	392.6

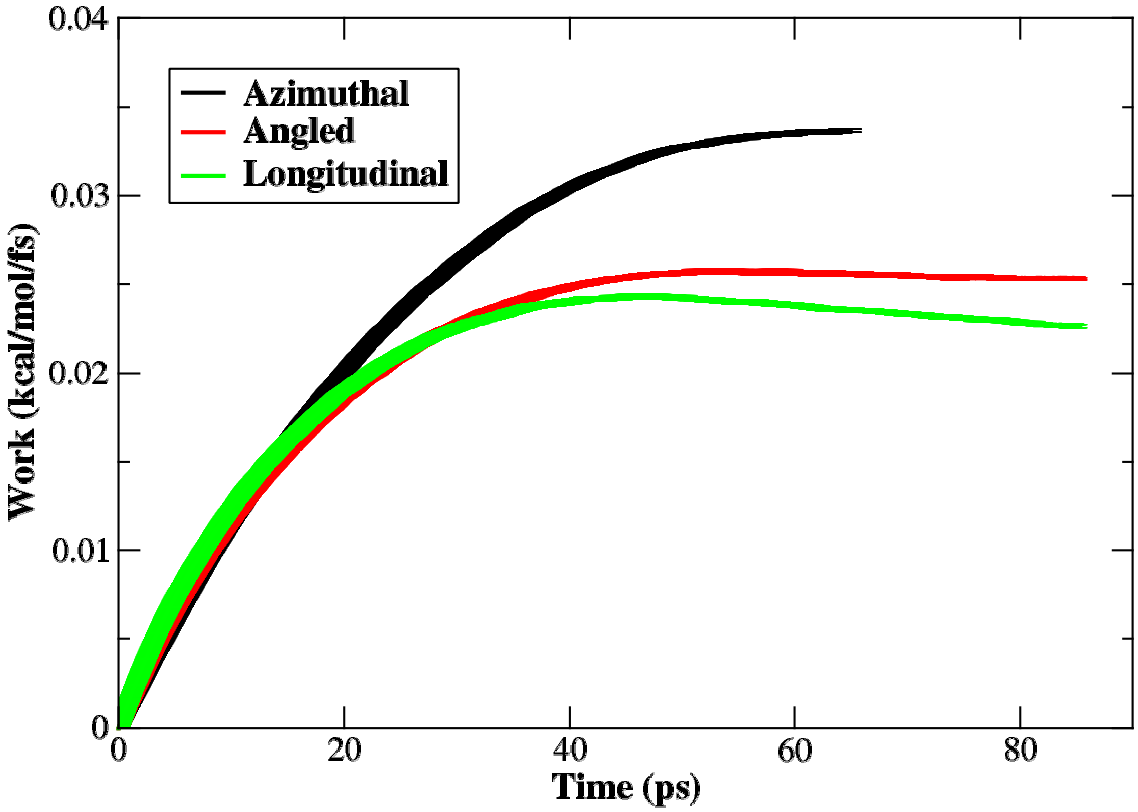

Figure S1: The calculated average work for the Tm transitions per quasirepeat from the 25 ps 2 stage SMD. The work shown is the work of the virtual spring for each time step, with the width of the curve representative of the standard error. The azimuthal has the highest initial barrier, but is the shortest transition. The longitudinal has the lowest barrier, with the angled slightly higher that the longitudinal, but both take longer to reach the target endpoints than the azimuthal.

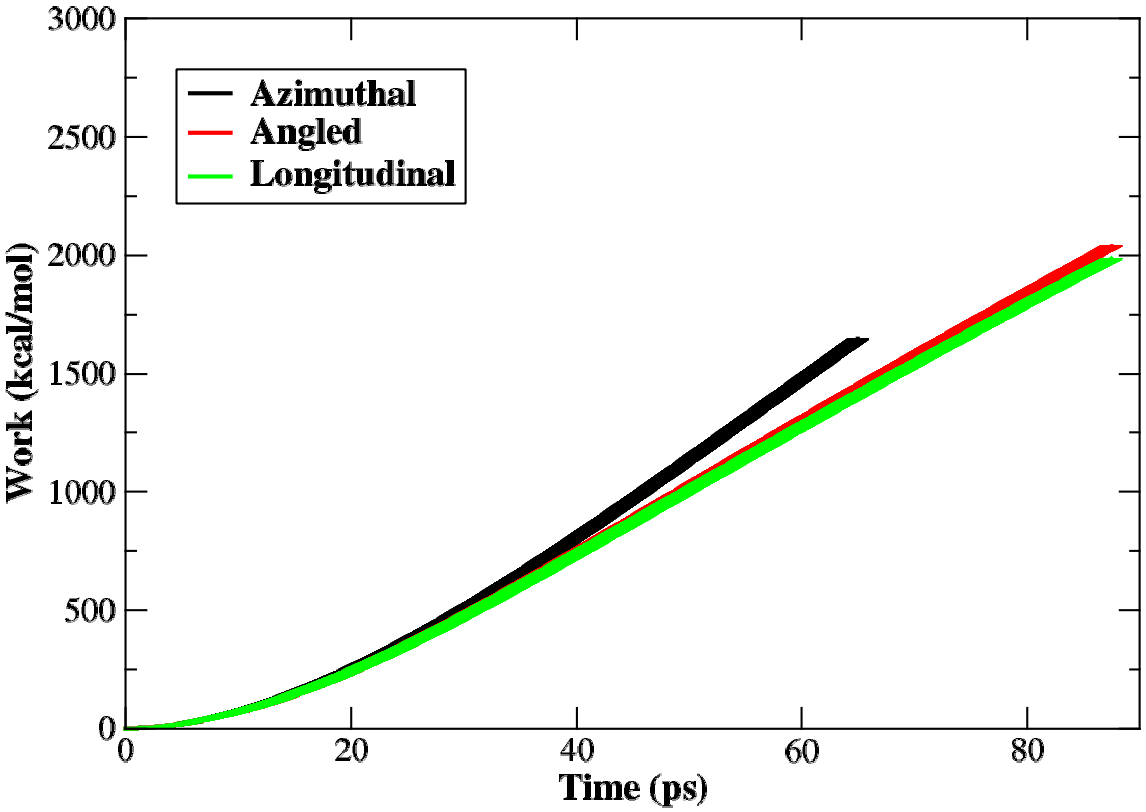

Figure S2: The average integrated total work for the Tm transitions per quasirepeat from SMD. The work shown is the total work of the virtual spring, with the width of the curve representative of the standard error. The azimuthal has the highest initial barrier, but is the shortest transition with the lowest total work. The longitudinal has the lowest initial barrier, with the angled slightly higher that the longitudinal, but both take longer to reach the target endpoints than the azimuthal resulting in larger total work.

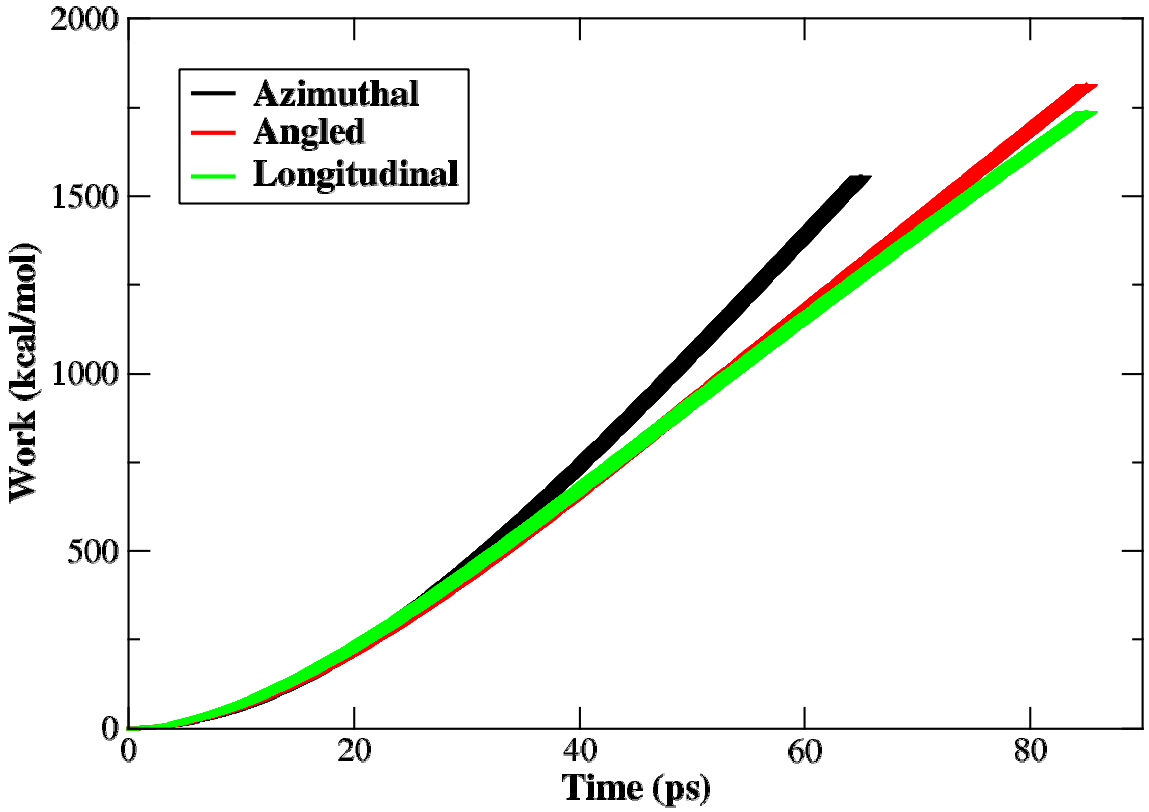

Figure S3: The average integrated total work for the Tm transitions per quasirepeat from the 25 ps 2 stage SMD. The work shown is the total work of the virtual spring, with the width of the curve representative of the standard error. The azimuthal has the highest initial barrier, but is the shortest transition with the lowest total work. The longitudinal has the lowest initial barrier, with the angled slightly higher that the longitudinal, but both take longer to reach the target endpoints than the azimuthal resulting in larger total work.

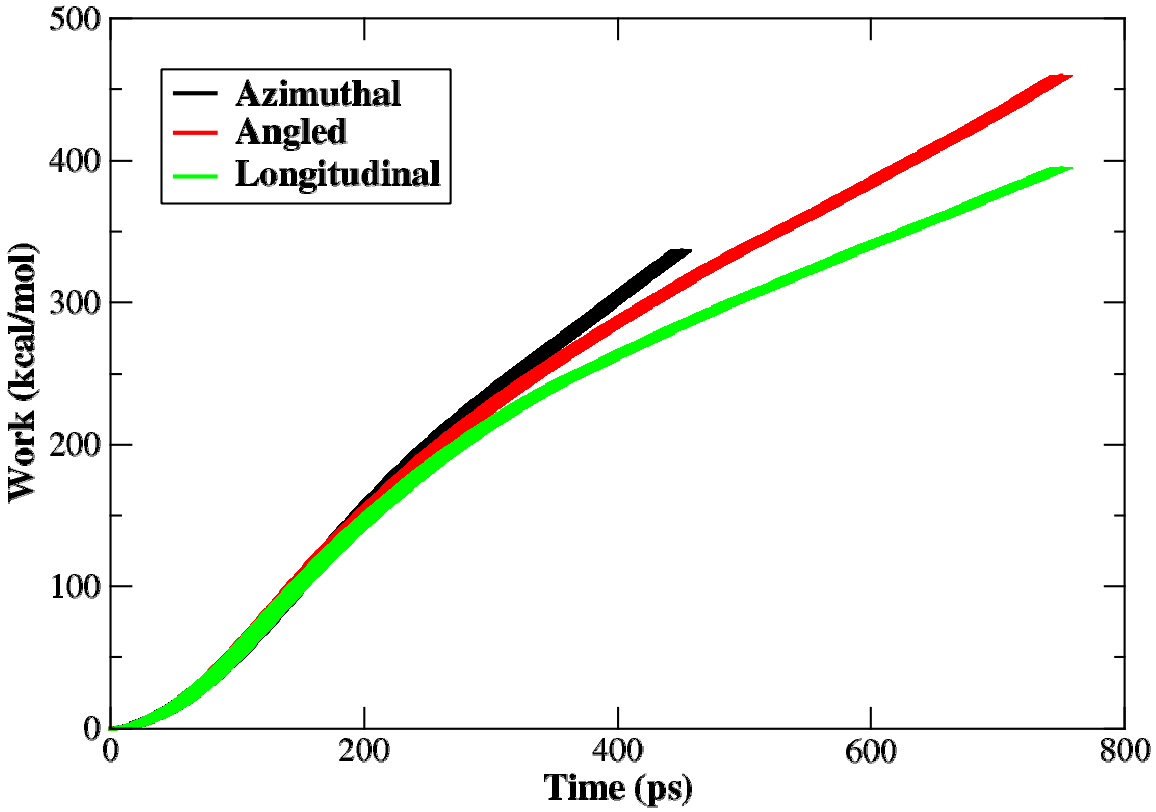

Figure S4: The average integrated total work for the Tm transitions per quasirepeat from slower SMD. The work shown is the total work of the virtual spring, with the width of the curve representative of the standard error. The azimuthal has the highest initial barrier, but is the shortest transition with the lowest total work. The longitudinal has the lowest initial barrier, with the angled slightly higher that the longitudinal, but both take longer to reach the target endpoints than the azimuthal resulting in larger total work.

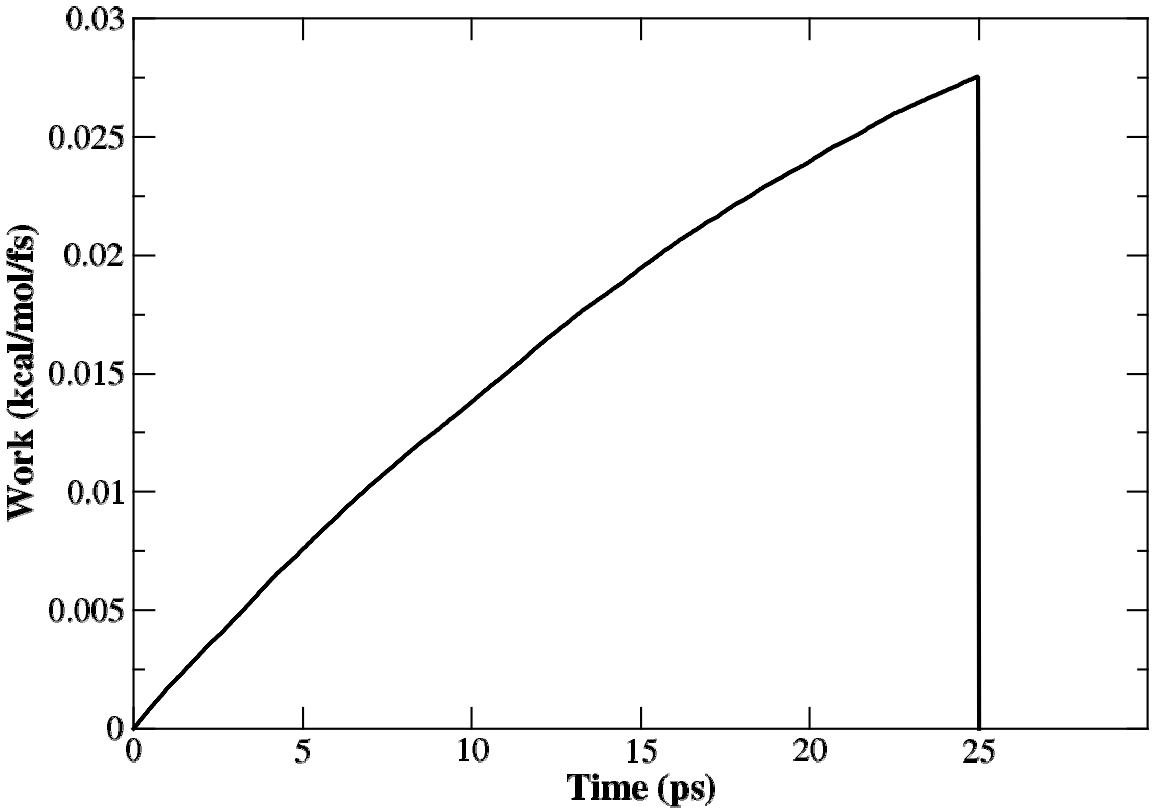

Figure S5: The calculated average work for the Tm transitions per quasirepeat for the 25 ps initial stage of the 2 stage SMD. The work shown is the work of the virtual spring for each time step, with the width of the curve representative of the standard error. Since the all of the transitions utilized the same perpendicular vectors for the first stage, the 3 transitions are equivalent. At 25 ps the work drops to zero because the forces were reset to zero to track the second stage of the transitions.

References

(1) Williams, M. R.; Lehman, S. J.; Tardiff, J. C.; Schwartz, S. D. Atomic resolution probe for allostery in the regulatory thin filament. *Proceedings of the National Academy of Sciences* **2016**, *113*, 3257–3262.

(2) Li, X. E.; Orzechowski, M.; Lehman, W.; Fischer, S. Structure and flexibility of the tropomyosin overlap junction. *Biochem Biophys Res Commun* **2014**, *446*, 304–308.

(3) Orzechowski, M.; Moore, J. R.; Fischer, S.; Lehman, W. Tropomyosin movement on F-actin during muscle activation explained by energy landscapes. *Archives of Biochemistry and Biophysics* **2014**, *545*, 63–68.

(4) Humphrey, W.; Dalke, A.; Schulten, K. VMD: visual molecular dynamics. *J Mol Graph* **1996**, *14*, 27–28,33–38.

(5) Phillips, J. C.; Braun, R.; Wang, W.; Gumbart, J.; Tajkhorshid, E.; Villa, E.; Chipot, C.; Skeel, R. D.; Kale, L.; Schulten, K. Scalable molecular dynamics with NAMD. *J Comput Chem* **2005**, *26*, 1781–1802.

(6) Brooks, B. R.; Brooks, C. L.; Mackerell, A. D.; Nilsson, L.; Petrella, R. J.; Roux, B.; Won, Y.; Archontis, G.; Bartels, C.; Boresch, S. et al. CHARMM: The biomolecular simulation program. *Journal of Computational Chemistry* **2009**, *30*, 1545–1614.

(7) Park, S.; Schulten, K. Calculating potentials of mean force from steered molecular dynamics simulations. *The Journal of Chemical Physics* **2004**, *120*, 5946–5961.

(8) Juraszek, J.; Vreede, J.; Bolhuis, P. G. Transition path sampling of protein conformational changes. *Chemical Physics* **2012**, *396*, 30–44.

(9) Von Der Ecken, J.; Müller, M.; Lehman, W.; Manstein, D. J.; Penczek, P. A.; Raunser, S. Structure of the F-actinâĂŞ âĂŞtropomyosin complex. *Nature* **2015**, *519*.

(10) von der Ecken, J.; Heissler, S. M.; Pathan-Chhatbar, S.; Manstein, D. J.; Raunser, S. Cryo-EM structure of a human cytoplasmic actomyosin complex at near-atomic resolution. *Nature* **2016**, *534*, 724–728.